masses contained in the polar vortex have been displaced from the pole toward the European continents during most of January 1992. The monthly mean January 1992 temperature at 30 mbar over the North Sea was 10 K lower than the 20-year (1965 to 1984) mean January values (K. Labitzke and B. Naujokat, *Beil. Berl. Wetterkarte* KNH1/1992). It remains to be established to what extent the low O_3 values observed over Europe are associated with this wave number 1 event or result from chemical destruction.

26. Discussions with J. Calvert, M. Coffey, and R. Garcia are gratefully acknowledged. The National Center for Atmospheric Research is sponsored by the National Science Foundation. C.G. is supported in part by the Gas Research Institute (contract 5090-254-1993) and by the Commission of the European Communities (Step Program).

6 April 1992; accepted 6 July 1992

Manganese Flux from Continental Margin Sediments in a Transect Through the Oxygen Minimum

Kenneth S. Johnson, William M. Berelson, Kenneth H. Coale, Teresa L. Coley, Virginia A. Elrod, W. Russell Fairey, Helen D. Iams, Tammy E. Kilgore, Jocelyn L. Nowicki

The flux of manganese from continental margin sediments to the ocean was measured with a free-vehicle, benthic flux chamber in a transect across the continental shelf and upper slope of the California margin. The highest fluxes were observed on the shallow continental shelf. Manganese flux decreased linearly with bottom water oxygen concentration, and the lowest fluxes occurred in the oxygen minimum zone (at a depth of 600 to 1000 meters). Although the flux of manganese from continental shelf sediments can account for the elevated concentrations observed in shallow, coastal waters, the flux from sediments that intersect the oxygen minimum cannot produce the subsurface concentration maximum of dissolved manganese that is observed in the Pacific Ocean.

Manganese is widely used as a model element for studies of redox chemical cycles in the sea. Insoluble manganese oxides are readily reduced to soluble Mn^{2+} by bacteria, photochemical reactions, and hydrothermal processes (*1*). Elevated concentrations of dissolved Mn are often evidence of active redox cycling. The processes controlling the oxidation states of a variety of other metals (for example, Ce, Co, and Cr) are interpreted by comparing their distributions with that of Mn (*2*).

Dissolved Mn profiles in the Pacific Ocean are characterized by maxima in the upper 100 m and wherever O_2 concentrations drop below 100 μM (*3*). The subsurface maximum is believed to be produced by the flux of dissolved Mn^{2+} from reducing sediments that intersect the O_2 minimum zone (*4–7*). However, there have been no direct measurements of the Mn flux from sediments along the continental margin, except in waters shallow enough to be reached by divers (*8, 9*). To test this hypothesis, we have directly measured the flux of Mn from sediments of the continental shelf and slope of the central California coastline using benthic chambers.

A well-developed O_2 minimum zone impinges on the continental margin between 600 and 1000 m along the central California coastline. Water column Mn concentrations in this zone are elevated twofold over background concentrations (Fig. 1). The flux of Mn from sediments that intersect this O_2 minimum was measured with a free-vehicle, benthic chamber (*10*) at depths from 95 to 1010 m along a transect near Point Piedras Blancas (35°40′N, 121°17′W). Similar benthic chambers have been used for studies of C and nutrient cycling in the deep sea (*11, 12*).

Manganese concentrations measured in benthic chambers deployed at all depths changed linearly with time (Fig. 2). Initial Mn concentrations in the chambers, determined from a straight line fitted to the data by least squares, were not significantly different ($P < 0.05$) from the corresponding ambient bottom water concentrations, which varied from 0.6 to 10 nM. There is no evidence of a change in the slope of a plot of Mn concentration versus time that would indicate enhanced release of the metal as O_2 concentrations decreased in the chambers (*13*). The benthic Mn flux calculated from these data is greatest at the shallowest sites, where O_2 levels in the overlying water are the highest, and the smallest Mn fluxes occurred in the O_2 minimum zone (Fig. 3A). The benthic Mn flux was proportional to the rate of O_2 consumption in the flux chambers (Fig. 3B).

A relation between benthic Mn and O_2 fluxes could be the result of several processes. Remineralization of organic C and release of bound metals could be limited by the flux of O_2 through a diffusive, benthic-boundary layer (*14*). To test this hypothesis, we performed an experiment at a site near the Los Angeles County sewage outfall at Whites Point where the rate of O_2 consumption was high and there was little sediment irrigation. Stirring rates in the benthic flux chambers were varied from 1.5 to 12 rpm, and no significant change was seen in the flux of O_2 or metals (*15*). Chambers were stirred at 6 rpm in the experiments shown here. Thus, we do not believe that benthic-boundary-layer hydrodynamics are responsible for the observed relation in metal and O_2 flux.

Changes in the rate of input of organic carbon to the sediments along the transect could link benthic Mn and O_2 fluxes. A positive relation between benthic Mn flux and primary production has been seen in experimental mesocosms (*16*). One hypothesis to account for this observation is that O_2 depletion and manganese oxide reduction occur in the near-surface sediments that receive the largest carbon input (*3*). Alternatively, trace metal fluxes could be controlled by release of bound metals, perhaps from particulate organic carbon (*17*) or calcium carbonate ($CaCO_3$) (*18*),

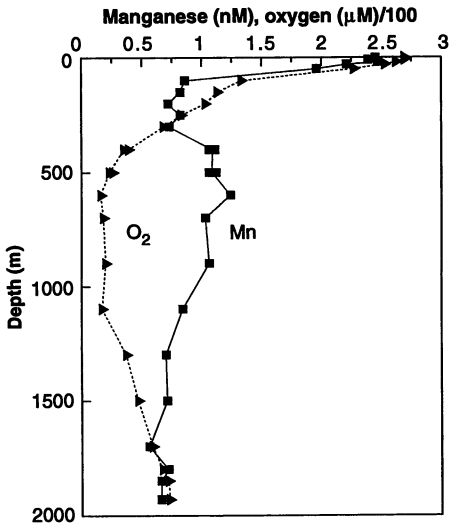

Fig. 1. Vertical profiles of dissolved Mn and O_2 from a hydrocast at 35°15′N, 121°52′W on 11 June 1991. Samples were collected with a General Oceanics Rosette sampler and 10-liter Niskin bottles. Manganese in each sample was determined at sea by flow injection analysis with chemiluminescence detection (FIA-CL) (*37*). The precision for replicate analyses was ±0.2 nM (90% confidence interval). Oxygen was determined by Winkler titration. Bottom depth is 2000 m.

K. S. Johnson, Moss Landing Marine Laboratories, Post Office Box 450, Moss Landing, CA 95039, and Monterey Bay Aquarium Research Institute, 160 Central Avenue, Pacific Grove, CA 93950.
W. M. Berelson, H. D. Iams, T. E. Kilgore, Department of Geological Sciences, University of Southern California, Los Angeles, CA 90089.
K. H. Coale, T. L. Coley, V. A. Elrod, W. R. Fairey, J. L. Nowicki, Moss Landing Marine Laboratories, Post Office Box 450, Moss Landing, CA 95039.

as the particles are remineralized under oxic conditions.

Several lines of evidence suggest that the Mn flux from sediments along the California coast is not driven by depletion of O_2 in the sediment and subsequent reduction of manganese oxides. First, the depth of O_2 penetration into the sediments was greatest at the shallowest sites (25 mm at a depth of 100 m versus 10 mm at 1010 m). We determined the O_2 profiles by measuring O_2 concentrations continuously with an amperometric electrode in the pore waters extruded from sediments with a whole-core squeezer (*19*). The data obtained in this manner are consistent with the results observed in this region with the use of microelectrodes (*20*). Although the shelf sediments receive the largest C input (*21*), they are overlain by water with the highest O_2 concentrations (Fig. 1). Therefore, Mn reduction should occur deeper in the sediments at the shallow sites. Second, the Mn flux appears to be produced by reactions occurring in the organic-rich layer of flocculent material at the sediment surface (fluff layer) where O_2 is present. Benthic fluxes of Mn, O_2, NO_3^-, Si, NH_4^+, and PO_4^{3-} calculated from concentration gradients in the interfacial sediments (*22*) all underestimate the fluxes observed with the benthic chamber at the stations on the shelf by factors of 5 to 25; yet these methods yield comparable fluxes for the deeper stations (for example, Fig. 3A). Irrigation of the sediments by benthic fauna is not likely to cause this bias. Irrigation rates that were estimated from ^{222}Rn fluxes and injections of an inert tracer (CsCl) into the flux chambers are not more than three times greater on the shelf than in the O_2 minimum, whereas the change in Mn flux is more than tenfold. In addition, Mn fluxes were not systematically related to the ^{222}Rn flux measured with the three replicate chambers at each station, as would be expected if irrigation produces the flux. Finally, estimates of the Mn flux produced by irrigation suggest that it accounts for at most 40% of the total benthic Mn flux (*23*). We hypothesize that O_2 consumption and remineralization of Mn and nutrients at the shelf stations occur primarily in a thin (<1 mm) fluff layer at the sediment surface. Similar results have been found in other studies of benthic chemical exchange from shallow sediments (*9, 24*).

The source of the Mn flux from the fluff layer remains problematic. Recent work has shown that reduction of manganese oxides can occur in the presence of O_2 (*25*). Reduction might also occur in anoxic microzones in the fluff layer, perhaps fecal pellets (*26*). We have no data that allow us to assess the role of manganese oxide reduction in the fluff layer. Instead we ask the question: Is there sufficient Mn in sinking particulate organic C or $CaCO_3$ to support the observed benthic flux? The flux of sinking C measured with sediment traps over an annual cycle at a depth of 50 m in Monterey Bay averaged 50 mmol m^{-2} day^{-1} (*27*). The ratio (on a mole basis) of organically bound Mn to organic C in particles collected by sediment traps deployed 90 km off this margin ranged from $(31 \pm 10) \times 10^{-6}$ (*18*) to $(58 \pm 36) \times 10^{-6}$ (*28*) (all error limits are the 90% confidence interval). Thus, the annual rain of organically bound Mn to the shelf sediments is about 2 μmol m^{-2} day^{-1} compared to an average benthic flux of 5 μmol m^{-2} day^{-1} (Fig. 3A). The C rain rate in Monterey Bay can be higher than the annual average by up to fourfold during upwelling events such as occurred on our cruise (surface nitrate concentrations regularly >15 μM). Clearly, enough Mn associated with organic matter can reach the sediments during high productivity periods to support the fluxes that we observed. However, the ratio of the benthic Mn flux to organic C oxidized (*29*) is $(890 \pm 560) \times 10^{-6}$. This ratio is significantly higher than that of the vertically falling particles, which suggests an additional Mn source.

Calcium carbonate may be an additional Mn source (*18*). Dissolution of $CaCO_3$ in sediments can be driven by CO_2 produced by respiration (*12, 30*). This process may occur even in sediments underlying waters supersaturated with respect to calcite (degree of saturation off central California at 100 m, $\Omega = 1.6$). We estimated the $CaCO_3$ dissolution flux in the sediments using the lander alkalinity, ammonia (NH_3), and total CO_2 data (*31*). The benthic Mn flux increased as the $CaCO_3$ dissolution flux increased (Fig. 3C). The ratio (on a mole basis) of the benthic Mn flux to C derived from $CaCO_3$ is between 2

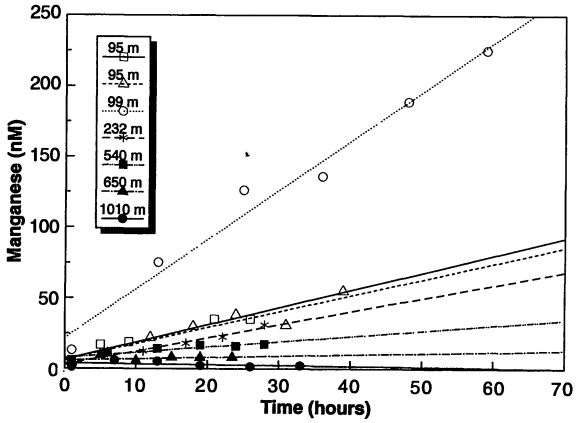

Fig. 2. Dissolved (<0.2 μm) Mn concentrations in the benthic flux chamber plotted versus the time interval between the closing of the chamber lid and sampling for deployments at seven sites. Each value is the average of the concentration obtained in the chambers that operated successfully. In most cases, all three chambers appeared to operate normally. The bottom depth at each site is shown on the figure. Sediments were incubated in situ under stirred chambers for 1 to 2 days: six aliquots of the overlying water were collected from each chamber. The first set of samples was usually collected 1 hour after the chamber lids closed, and the last was collected 1 hour before the vehicle left the bottom. All samples were analyzed on board ship by FIA-CL (*37*) after the samples were diluted 1 + 7.5 with ultrapure water. Precision on these samples is ±2 nM.

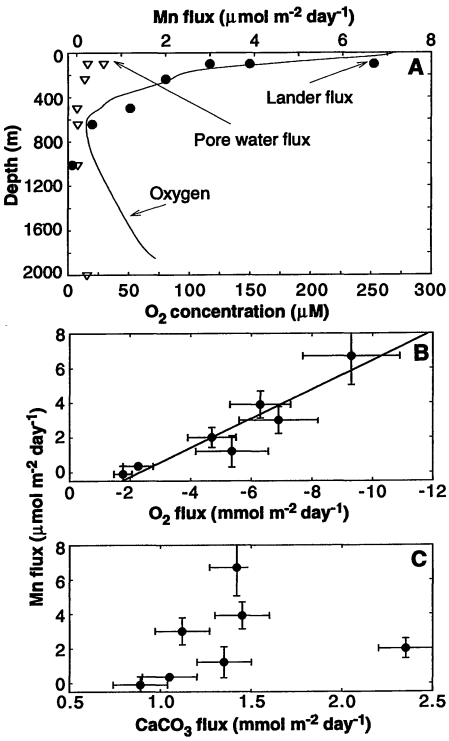

Fig. 3. (**A**) Benthic Mn flux and O_2 concentration in the water column plotted versus depth. Benthic flux values derived from the lander and by modeling pore water gradients of Mn are shown. (**B**) Plot of Mn flux versus O_2 flux into the sediments. Oxygen concentrations in the chambers were monitored continuously with an amperometric electrode operated in the pulsed mode (*38*). Errors for the flux measurements (1 SD) were determined from the replicate chamber measurements if results for more than one chamber were available, or from the error in the slope of the regression line fitted to the concentration versus time data combined with the 15% error in determining the chamber volumes if only one chamber functioned. (**C**) Plot of Mn flux versus the estimated rate of $CaCO_3$ dissolution.

$\times 10^{-3}$ and 10×10^{-3}. The ratio of Mn to C bound by $CaCO_3$ in sinking material ranges from 2×10^{-3} to 27×10^{-3} (*18*). Thus, sufficient Mn should be transported to the sediments with $CaCO_3$ if the inorganic C flux is one half of the vertical flux of organic C (*32*).

Our evidence suggests that there is potentially enough Mn associated with the particulate organic C and $CaCO_3$ that reaches the sediment surface to support the benthic fluxes. We cannot preclude a role for manganese oxide reduction in generating the flux, but it must occur in the oxic sediments near the sediment-water interface. Dissolved Mn(II) that is produced in the O_2-deficient region below the sediment-water interface appears to be reprecipitated in surficial sediments when the bottom water O_2 is >10 μM (*33*). Apparently, only the Mn released at the sediment-water interface can escape from the sediments.

All of the processes discussed above that might control Mn flux from the sediments (respiration, $CaCO_3$ dissolution, or manganese oxide reduction) are linked to the availability of organic C. Carbon flux through the water column decreases rapidly with depth (*21*), as does the flux of organically bound Mn (*28*). Low benthic fluxes of Mn measured in the O_2 minimum zone are likely to reflect the low influx of organic C and organically bound Mn in this depth range. It should not be surprising, therefore, that the lowest fluxes of Mn were found in the O_2 minimum zone.

High Mn concentrations (>5 nM) in the mixed layer are regularly observed near the coast (*6, 28, 34*). The loss of Mn from the mixed layer due to offshore diffusion for this section of the central California coast was calculated to range from 0.005 to 57 nmol liter^{-1} year^{-1} (*35*). The input rate of Mn calculated from the flux of Mn at 100 m (Fig. 3A) for an assumed mean depth over the shelf of 50 m is 44 nmol liter^{-1} year^{-1}. The highest loss rates are comparable to the input rate, and they would require that each Mn atom be recycled from the water to the sediment only once before removal from the shelf to the open ocean (*35*). However, this high offshore flux requires a much greater lateral gradient over the shelf than has been observed. The lower loss rates, which are consistent with the observed gradients, would require that each Mn atom be recycled from the shelf sediments to the water column many times before export to the open sea. Such recycling would account for the large concentrations observed in this region. This mechanism should be representative of the processes that control Mn concentration over all continental shelves.

The Mn concentration maximum in the O_2 minimum zone off California is not a result of an enhanced flux from the sediments. Thus, this maximum must be generated in the water column, but the mechanism is not clear. Reduction of manganese oxides on particles falling through the water column in the O_2 minimum zone (*3*) and remineralization of Mn bound by particulate organic C (*34*) have been suggested as possible mechanisms that might support the Mn maximum. The maximum could also be produced by a reduction in the rate of Mn scavenging in the O_2 minimum (*36*). Further research must focus on these processes.

REFERENCES AND NOTES

1. R. C. Myers and K. H. Nealson, *Science* **240**, 1319 (1988); W. G. Sunda and S. A. Huntsman, *Deep-Sea Res.* **35**, 1297 (1988); K. L. Von Damm *et al.*, *Geochim. Cosmochim. Acta* **49**, 2197 (1985).
2. E. R. Sholkovitz and D. L. Schneider, *Geochim. Cosmochim. Acta* **55**, 2737 (1991); G. A. Knauer, J. H. Martin, R. M. Gordon, *Nature* **297**, 49 (1982); J. W. Murray, B. Spell, B. Paul, in *Trace Metals in Sea Water*, C. S. Wong *et al.*, Eds. (Plenum, New York, 1983), pp. 643–670.
3. G. P. Klinkhammer and M. L. Bender, *Earth Planet. Sci. Lett.* **46**, 361 (1980).
4. W. M. Landing and K. W. Bruland, *ibid.* **49**, 45 (1980).
5. J. H. Martin and G. A. Knauer, *ibid.* **67**, 35 (1984).
6. C. J. Jones and J. W. Murray, *Limnol. Oceanogr.* **30**, 81 (1985).
7. J. H. Martin and G. A. Knauer, *Nature* **314**, 524 (1985).
8. W. Balzer, *Geochim. Cosmochim. Acta* **46**, 1153 (1982).
9. B. Sundby *et al.*, *ibid.* **50**, 1281 (1986).
10. The free vehicle lander [W. M. Berelson and D. E. Hammond, *Deep-Sea Res.* **33**, 1439 (1986)] has three cylindrical chambers, each of which covers an area of 720 cm^2 and incubates a volume of 5 to 9 liters. The chamber water was continuously stirred with a paddle at a rate (6 rpm) determined to create a diffusive boundary layer 200 to 400 μm thick (*12*). Six samples were drawn from each chamber, and the measured concentrations were corrected for the inflow of ambient bottom water that takes place during sampling. The corrected sample concentrations were fitted to a linear regression line (corrected concentration versus sample time), and the flux was calculated from the slope. The chamber volume was established by measurement of the dilution of a CsCl spike injected into the chamber before the fourth sample draw.
11. W. M. Berelson, D. E. Hammond, K. S. Johnson, *Geochim. Cosmochim. Acta* **51**, 1345 (1987).
12. W. M. Berelson, D. E. Hammond, G. A. Cutter, *ibid.* **54**, 3013 (1990).
13. Although none of the chambers became anoxic during the course of the incubation, the O_2 concentration did decrease in some chambers to a final value that was 15% of the initial concentration. We looked carefully at all the data and see no cases where the Mn flux appeared to increase over the course of the incubation. The O_2 decrease was approximately linear. The pH did not change by more than 0.2 during the duration of an incubation.
14. P. H. Santschi, R. F. Anderson, M. Q. Fleisher, W. Bowles, *J. Geophys. Res.* **96**, 10641 (1991).
15. Chambers were stirred at rates of 1.5, 6, and 12 rpm. The corresponding Mn fluxes were: 8 ± 6, 18 ± 4, and 18 ± 5 μmol m^{-2} day^{-1}; the corresponding O_2 fluxes were 15 ± 4, 21 ± 5, and 24 ± 6 mmol m^{-2} day^{-1}. Errors are 90% confidence limits.
16. C. D. Hunt, *Limnol. Oceanogr.* **28**, 913 (1983).
17. R. Collier and J. Edmond, *Prog. Oceanogr.* **13**, 113 (1984).
18. J. H. Martin and G. A. Knauer, *Deep-Sea Res.* **30**, 411 (1983).
19. M. L. Bender *et al.*, *Limnol. Oceanogr.* **32**, 1214 (1987).
20. R. A. Jahnke, C. E. Reimers, D. B. Craven, *Nature* **348**, 50 (1990).
21. J. H. Martin, G. A. Knauer, D. M. Karl, W. W. Broenkow, *Deep-Sea Res.* **34**, 267 (1987).
22. Pore water samples for metal analysis were obtained with a vertical resolution of 1 mm to a depth of 30 mm with use of the whole core squeezer. Preservation of a near-surface Mn maximum in the profiles that is associated with the disappearance of dissolved O_2 and a minimum in pH indicates that chromatographic effects have not smeared out the metal signal [R. Fairey *et al.*, *Eos* **42**, 265 (1991)].
23. The estimate of the irrigation flux was based on an irrigation velocity of 0.6 ± 0.3 cm day^{-1}, derived from the ^{222}Rn measurements, and an Mn concentration of 400 nM at a depth of 3 cm in the sediments that is typical of the values observed on the shelf.
24. G. T. Rowe and A. P. McNichol, *Geochim. Cosmochim. Acta* **55**, 2989 (1991); J. P. Sweerts, J. W. M. Rudd, C. A. Kelly, *Limnol. Oceanogr.* **31**, 330 (1986).
25. B. M. Tebo, R. A. Rosson, K. H. Nealson, in *Black Sea Oceanography*, E. Izdar and J. W. Murray, Eds. (Kluwer, Dordrecht, Netherlands, 1991), pp. 173–185; W. C. Ghiorse, in *Biology of Anaerobic Microorganisms*, A. J. B. Zehnder, Ed. (Wiley-Interscience, New York, 1988), pp. 305–331.
26. A. L. Alldredge and Y. Cohen, *Science* **235**, 689 (1987).
27. F. P. Chavez *et al.*, paper presented at the second meeting of the Oceanography Society, St. Petersburg, FL, 25 to 28 March 1991.
28. J. H. Martin, G. A. Knauer, W. W. Broenkow, *Deep-Sea Res.* **32**, 1405 (1985).
29. The amount of organic C oxidized was determined from a budget of total inorganic C, O_2, NO_3^-, NH_3, and alkalinity fluxes (*11, 12*).
30. S. Emerson and M. Bender, *J. Mar. Res.* **39**, 139 (1981).
31. Procedures for estimating $CaCO_3$ dissolution are described in (*11, 12*). Some of the alkalinity flux is due to NH_3 (<10%) and some is due to sulfate reduction and precipitation of pyrite (10 to 20%). The NH_3 contribution was measured; we estimated the amount of sulfate reduction by assuming values for the percent of S in the sediments and using reported sediment accumulation rates (C. Reimers, R. Jahnke, D. McCorkle, *Glob. Biogeochem. Cycles*, in press). The stations were grouped by depth, and it was assumed that the percent of S in sediments increased from 0.5 to 1.2 as depth increased from 100 to 1000 m. These values are based on literature values of S in sediments [B. W. Leslie, thesis, University of Southern California, Los Angeles (1989)]. We assumed that the S was present as pyrite [I. R. Kaplan *et al.*, *Geochim. Cosmochim. Acta* **27**, 297 (1963)]. The sulfate reduction rates derived from these data are consistent with estimates from earlier studies in this area (*20*). The largest source of error in determining $CaCO_3$ dissolution rates is in the alkalinity flux data, which has an uncertainty of 10 to 50%.
32. S. Honjo, S. J. Manganini, J. J. Cole, *Deep-Sea Res.* **29**, 609 (1982).
33. T. J. Shaw, J. M. Gieskes, R. A. Jahnke, *Geochim. Cosmochim. Acta* **54**, 1233 (1990).
34. W. M. Landing and K. W. Bruland, *ibid.* **51**, 29 (1987).
35. We calculated the removal rate as the product of the second derivative of the Mn concentration with respect to distance from the coast and the horizontal eddy diffusion coefficient using the data reported by Landing and Bruland (*34*). They fitted their Mn measurements in surface water (units of nanomoles per kilogram) to the equation; ln Mn = 4.5 − 0.63 ln X, where X is the distance offshore (in kilometers), and obtained a removal rate of 53 nmol liter^{-1} year^{-1} at a distance of 10 km from the coast. However, this equation extrapolates to a

Mn concentration of 93 nM over the shelf, which is never observed. The equation ln Mn = 5.4 − 0.002 X provides a good fit to data from within 500 km of the coast. The offshore transport term calculated from this equation is 0.005 nmol liter^{-1} year^{-1}.
36. K. S. Johnson, *Eos* **71**, 89 (1990).
37. T. P. Chapin, K. S. Johnson, K. H. Coale, *Anal. Chim. Acta* **249**, 469 (1991).
38. C. Langdon, *Deep-Sea Res.* **31**, 1357 (1984).
39. This work was supported by National Science Foundation grants OCE8923057 (K.S.J. and K.H.C.) and OCE8923024 (W.M.B.) and Office of Naval Research grant N00014-89-J-1070. We thank the officers and crew of the R/V *Pt. Sur* for their assistance.

3 April 1992; accepted 25 June 1992

Tentoxin Sensitivity of Chloroplasts Determined by Codon 83 of β Subunit of Proton-ATPase

Adi Avni,* James D. Anderson,† Neta Holland, Jean-David Rochaix, Zippora Gromet-Elhanan, Marvin Edelman

Tentoxin is a naturally occurring phytotoxic peptide that causes seedling chlorosis and arrests growth in sensitive plants and algae. In vitro, it inhibits activity of the β subunit of the plastid proton–adenosine triphosphatase (ATPase) from sensitive species. Plastid *atp*B genes from six closely related, tentoxin-sensitive or -resistant *Nicotiana* species differ at codon 83, according to their response to the toxin: glutamate correlated with resistance and aspartate correlated with sensitivity. The genetic relevance of this site was confirmed in *Chlamydomonas reinhardtii* by chloroplast transformation. The alga, normally tentoxin-resistant, was rendered tentoxin-sensitive by mutagenesis of its plastid *atp*B gene at codon 83. Codon 83 may represent a critical site on the β subunit that does not compete with nucleotide binding or other catalytic activities.

Tentoxin, a cyclic tetrapeptide [cyclo L-leucyl-*N*-methyl-(Z)-dehydrophenyl-alanyl-glycyl-*N*-methyl-alanyl] (*1*), is a phytotoxin produced by the fungus *Alternaria tenuis*. The diversity of effects in a variety of plants suggests multiple modes and sites of action (*2*). Tentoxin prevents chlorophyll accumulation in germinating seedlings of some, but not all, angiosperms (*3*), an effect termed "chlorosis" (*4*). Chlorosis was claimed to arise from interference with transport or integration of specific nuclear-coded proteins into the developing plastid of sensitive, but not resistant, species (*5, 6*). However, tentoxin is also a potent inhibitor of energy transfer at the terminal step in photophosphorylation in isolated plastid membranes (*7*) and inhibits light-driven, but not adenosine triphosphate (ATP)–driven, protein and RNA synthesis in isolated chloroplasts (*8*). Thus, chlorosis, a cytoplasmically inherited chloroplast character (*9, 10*), may result from inhibition of photophosphorylation by interaction of tentoxin with a specific site on the coupling factor (CF_1) of the plastid proton-ATPase in sensitive species (*11*). Binding studies and ATPase inhibition kinetics show that, in sensitive species, tentoxin binds tightly to a single site on chloroplast-encoded α or β subunits of CF_1 (*12*). This binding is uncompetitive with respect to ATP and adenosine diphosphate (ADP) (*13*).

We used the β-less *Rhodospirillum rubrum* chromatophore system (*14*) to determine which of the two CF_1 subunits interacts with tentoxin (*15*). This system requires addition of β subunit and trace amounts of α subunit for restoration of ATPase activity (*16*). The external source of α subunit was, in all cases, from lettuce, a tentoxin-sensitive species (*17*). Heterologously reconstituted chromatophores proved sensitive to tentoxin when purified β subunit from a tentoxin-sensitive species [*Nicotiana tabacum* line 92 (*18*) or lettuce] was used. However, chromatophores were resistant to >100-fold higher concentrations of tentoxin when purified β subunit from a tentoxin-resistant species [*Nicotiana tabacum* var. *Xanthi* (*18*)] was used (Fig. 1). Thus, the response of the reconstituted chromatophores to tentoxin depended on the source of CF_1-β.

The peptide sequence identity among CF_1-β subunits from a variety of higher plants is 92 to 95% (*19*). We therefore reasoned that within a single genus, such as *Nicotiana* [where out of 40 species tested, 9 are tentoxin-resistant and 31 are tentoxin-sensitive (*3, 18*)], CF_1-β sequence variation might be limited enough that a unique difference could be identified between resistant and sensitive plants. Accordingly, the *atp*B coding regions from two resistant (R) and three sensitive (S) *Nicotiana* species [*N. tabacum* var. *Xanthi* (R), *N. rustica* (R), *N. bigelovii* (S), *N. plumbaginifolia* (S), and *N. tabacum* line 92 (S)] were cloned, were sequenced (*20*), and were compared with that of *N. tabacum* var. BY4 (R) (*21*). Homology among the six genes and among the proteins they encode was >99% (Fig. 2). Between CF_1-β of *N. tabacum* var. *Xanthi* and that of *N. bigelovii*, only a single amino acid difference was found: glutamate (E) or aspartate (D) at residue 83. All three sensitive lines had D at position 83 and all three resistant lines had E.

We transformed chloroplasts of *Chlam-*

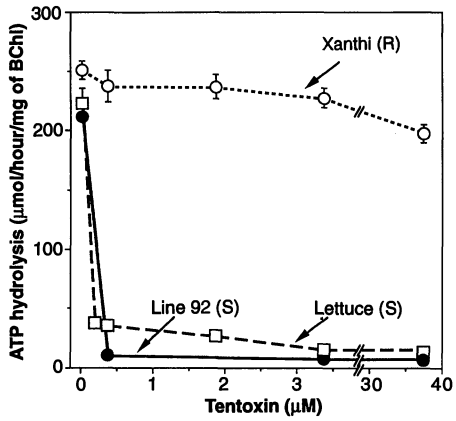

Fig. 1. The effect of tentoxin on ATP hydrolysis in reconstituted *Rhodospirillum rubrum* chromatophores. Photosynthetic membranes (*36*) were prepared from *Nicotiana* and lettuce, and were extracted with 2 M LiCl and 4 mM MgATP (*16*). CF_1 fractions were purified from the LiCl supernatant by anion-exchange chromatography on a fast protein liquid chromatography (FPLC) Mono Q column (*16*) to yield CF_1-β immunologically free of CF_1-α (purified-β), and a fraction containing both CF_1-α and CF_1-β in a ratio of ~1:1 (purified-αβ). Reconstitution of β-less chromatophores was carried out as detailed (*16*), with 3 μg of purified-αβ from lettuce, Lettuce (S); 3 μg of purified-β from *N. tabacum* var. *Xanthi* plus 0.4 μg of purified-αβ from lettuce, Xanthi (R); or 3 μg of purified-β from *N. tabacum line 92* plus 0.4 μg of purified-αβ from lettuce, Line 92 (S) (*30*). Samples were incubated with β-less *R. rubrum* chromatophores (*14*), and the specific rate of ATP hydrolysis determined in the presence of increasing tentoxin concentration. (R) = tentoxin-resistant and (S) = tentoxin-sensitive species as determined by the seedling test (*37*); BChl = bacterial chlorophyll, determined according to Clayton (*38*).

A. Avni, J. D. Anderson, N. Holland, M. Edelman, Department of Plant Genetics, Weizmann Institute of Science, Rehovot 76100, Israel.
J.-D. Rochaix, Department of Molecular Biology, University of Geneva 30, Quai Ernest Ansernet, CH-1211 Geneva, Switzerland.
Z. Gromet-Elhanan, Department of Biochemistry, Weizmann Institute of Science, Rehovot 76100, Israel.

*Present address and to whom correspondence should be addressed: Plant Molecular Biology Laboratory, U.S. Department of Agriculture, Agricultural Research Service (USDA/ARS) Beltsville Agricultural Research Center, Building 006, Beltsville, MD 20705.
†On leave from Plant Hormone Laboratory, USDA/ARS, Beltsville, and present address: Weed Science Laboratory, USDA/ARS, Beltsville Agricultural Research Center, Beltsville, MD 20705.